

NAVAL POSTGRADUATE SCHOOL

Monterey, California



THESIS

**PROPAGATION OF FIRE GENERATED SMOKE
AND HEAT TRANSFER IN SHIPBOARD
SPACES WITH A HEAT SOURCE**

by

Billy J. Vegara

September 2000

Thesis Advisor:

M.D. Kelleher

Approved for public release; distribution is unlimited.

REPORT DOCUMENTATION PAGE		Form Approved OMB No. 0704-0188	
Public reporting burden for this collection of information is estimated to average 1 hour per response, including the time for reviewing instruction, searching existing data sources, gathering and maintaining the data needed, and completing and reviewing the collection of information. Send comments regarding this burden estimate or any other aspect of this collection of information, including suggestions for reducing this burden, to Washington Headquarters Services, Directorate for Information Operations and Reports, 1215 Jefferson Davis Highway, Suite 1204, Arlington, VA 22202-4302, and to the Office of Management and Budget, Paperwork Reduction Project (0704-0188) Washington DC 20503.			
1. AGENCY USE ONLY (Leave blank)	2. REPORT DATE September 2000.	3. REPORT TYPE AND DATES COVERED Master's Thesis	
4. TITLE AND SUBTITLE: Propagation of Fire Generated Smoke in Shipboard Spaces with Heat Source.		5. FUNDING NUMBERS	
6. AUTHOR(S) Vegara, Billy J.			
7. PERFORMING ORGANIZATION NAME(S) AND ADDRESS(ES) Naval Postgraduate School Monterey CA 93943-5000		8. PERFORMING ORGANIZATION REPORT NUMBER	
9. SPONSORING/MONITORING AGENCY NAME(S) AND ADDRESS(ES)		10. SPONSORING/MONITORING AGENCY REPORT NUMBER	
11. SUPPLEMENTARY NOTES The views expressed here are those of the authors and do not reflect the official policy or position of the Department of Defense or the U.S. Government.			
12a. DISTRIBUTION/AVAILABILITY STATEMENT Approved for public release; distribution is unlimited.		12b. DISTRIBUTION CODE	
13. ABSTRACT (maximum 200 words) The propagation of fire generated smoke and heat transfer into a shipboard space has been computationally modeled using a commercial code generated by Computational Fluid Dynamics Research Corporation (CFDRC). The space modeled was 1-158-1-L of an Arleigh Burke Class Flight IIA Destroyer. Three smoke and heat scenarios are applied to the space. For all three scenarios, the inlet used is the forward, inboard watertight door. Smoke enters the upper half of the door, while air enters through the bottom half. The temperature of the inlet fluids is altered to observe its effect on propagation. In the last scenario, the floor temperature is isothermally held at 1200 K to simulate a fire in the space below. The results of this scenario shows that extreme temperatures of adjacent spaces has minimal effect on propagation. The overall goal of this study is to show how computational methods can be used to model propagation of smoke in shipboard spaces.			
14. SUBJECT TERMS Convection, Smoke Modeling, Computational Fluid Dynamics		15. NUMBER OF PAGES 97	
16. PRICE CODE			
17. SECURITY CLASSIFICATION OF REPORT Unclassified	18. SECURITY CLASSIFICATION OF THIS PAGE Unclassified	19. SECURITY CLASSIFICATION OF ABSTRACT Unclassified	20. LIMITATION OF ABSTRACT UL

THIS PAGE INTENTIONALLY LEFT BLANK

Approved for public release; distribution is unlimited

**PROPAGATION OF FIRE GENERATED SMOKE IN SHIPBOARD SPACES WITH
HEAT SOURCE**

Billy J. Vegara
Lieutenant, United States Navy
B.S., Southern University and A&M College, 1992

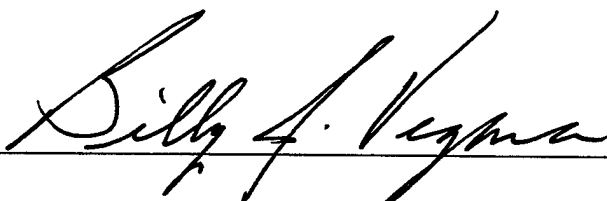
Submitted in partial fulfillment of the
requirements for the degree of

MASTER OF SCIENCE IN MECHANICAL ENGINEERING

from the

NAVAL POSTGRADUATE SCHOOL
September 2000

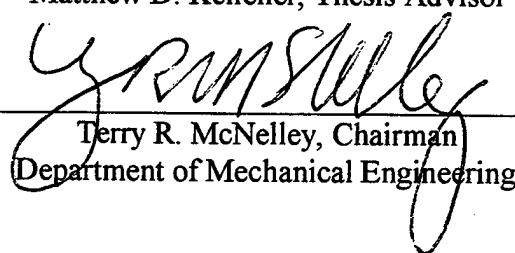
Author:



Approved by:



Matthew D. Kelleher, Thesis Advisor



Terry R. McNelley, Chairman
Department of Mechanical Engineering

THIS PAGE INTENTIONALLY LEFT BLANK

ABSTRACT

The propagation of fire generated smoke into a shipboard space has been computationally modeled using a commercial code generated by Computational Fluid Dynamics Research Corporation (CFDRC). This study was based on space 01-163-2-L of an Arleigh Burke Class Flight IIA Destroyer. However, with changes, the model can be reconfigured to represent other shipboard spaces. Multiple smoke scenarios are applied to the space. For all scenarios, the inlet used is forward watertight door. Smoke enters the upper half of the door, while air enters through the bottom half. The temperature of the inlet fluids is altered to observe its effect on propagation. In the last scenario, the floor temperature is isothermally held at 1200 K to simulate a fire in the space below. The results of this scenario shows that extreme temperatures of adjacent spaces has minimal effect on propagation. The overall goal of this study is to show how computational methods can be used to model propagation of smoke in shipboard spaces.

THIS PAGE INTENTIONALLY LEFT BLANK

TABLE OF CONTENTS

I.	INTRODUCTION.....	1
	A. BACKGROUND.....	1
	B. DESCRIPTION OF THE PROBLEM.....	4
	C. PREVIOUS WORK.....	5
	D. OBJECTIVES.....	7
II.	COMPUTATIONAL FLUID DYNAMICS	9
	A. OVERVIEW.....	9
	B. FINITE VOLUME METHOD.....	10
	1. Basic Governing Equations.....	10
	2. Discretization Methods.....	11
III.	MODEL.....	15
	A. GEOMETRY.....	15
	1. Model Selection.....	15
	2. Grid Distribution and Model Generation.....	18
	B. THERMOPHYSICAL MODEL.....	23
	C. ADDITIONAL INPUTS.....	24
IV.	RESULTS.....	25
V.	CONCLUSIONS.....	27
VI.	RECOMMENDATIONS.....	28
	APPENDIX A.....	29
	APPENDIX B.....	38

APPENDIX C.....	47
LIST OF REFERENCES.....	54
INITIAL DISTRIBUTION LIST.....	56

ACKNOWLEDGEMENT

I would like to thank Professor Kelleher for his patience and guidance during the completion of this thesis. The combination of his expertise as a researcher and his tolerance as a teacher made this experience very rewarding. Additionally, I would like to thank Dr. Evangelos Hytopoulos of the CFD Research Corporation, West Coast Branch. His help with my model was invaluable, and he also gave me a “crash” course on CFD-ACE+ Version 6.2, after I had done much of my thesis work on Version 5.0.

THIS PAGE INTENTIONALLY LEFT BLANK

I. INTRODUCTION

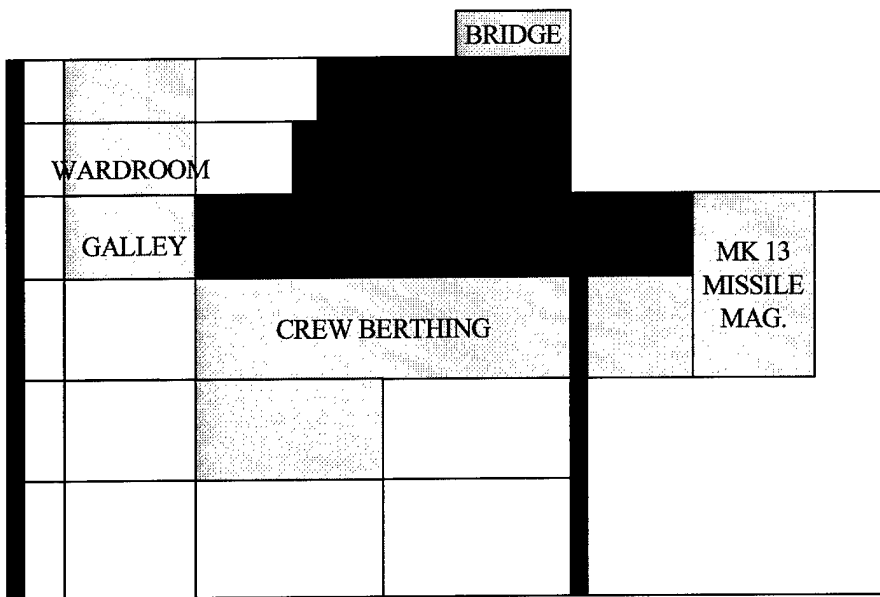
A. BACKGROUND

On May 17, 1987, the USS *Stark* (FFG-31) was hit by two French-built AM-39 Exocet missiles fired from an Iraqi F-1 Mirage jet aircraft. The first missile punctured the hull of the ship and failed to detonate. However, it was later determined that the first missile caused the majority of the damage suffered by the *Stark* due to the amount of burning missile propellant it left in its wake. The second missile hit the ship eight feet from the first missile and exploded three to five feet (0.9 to 1.5 meters) inside the hull. During the subsequent investigation of the *Stark* incident, it was estimated that each missile carried 300 pounds (136 kilograms) of propellant into the ship-control department berthing and the chief petty officers' mess. The propellant for the Exocet missile burns at 3,000 to 5,000 degrees Fahrenheit (1900 to 3000 Kelvin); it contains its own oxidizer to ensure complete burning and maximum heat release. [Ref 1]

The propellant-induced fires onboard the *Stark* resulted in smoke and heat far exceeding any conditions which could be simulated by training evolutions. Even though the *Stark* was fortunate that both missiles did not detonate, this modern warship, equipped with a state of the art damage control system and manned by a well-trained crew, still suffered significant damage due to the large amounts of smoke and heat caused by the missile propellant. See Figure 1.

It is this type of fire causing extreme temperatures and huge amounts of smoke that is the focus of this study. Specifically, this paper will address the movement of smoke through a main shipboard passageway, taking into account buoyancy effects

caused by variable densities and gravity forces. In addition, a heat source will be placed adjacent to one of the walls of the passageway in order to study the effects of a fire adjacent to the space.



- FIRE BOUNDARY
- SMOKE/HEAT DAMAGE
- FIRE DAMAGE

**Figure 1. USS Stark (FFG-31). Summary of Damage, Starboard View.
From Ref. [1].**

B. DESCRIPTION OF PROBLEM

Essential to the design of ships is the complex problem of predicting the shipboard environment during an intense fire. As ships become more costly to construct, it is imperative that current technology be utilized in order to construct a superior ship. Naval engineers must employ the increased capabilities of computer processors and the numerous fluid flow analysis software packages to develop improved warship designs.

In the past, the designing of ships and their damage control systems has been based on lessons learned from prior conflagrations onboard Navy ships. Ships built as recently as the 1980's employed designs developed during World War II. With current technology, many vital spaces of a ship could be modeled on a computer and then undergo multiple damage control scenarios in order to validate the design of the ship's damage control capabilities. Problems with the ship design can be changed and improved even before the ship progresses from the design stage.

Computer modeling can also be used to test damage control doctrine. Fluid flow software can be used to analyze smoke propagation and even the propagation of the fallout of a chemical, biological, or nuclear attack. Using the information from these simulations, Department of the Navy analysts can develop the damage control doctrine well before the keel of the ship is laid.

Service chiefs have approved the Mission-Needs Statement for the next-generation DD-21 Land Attack Destroyer which requires it to operate, fight, and survive with a crew of just 95 sailors, with remote sensors and automated systems expected to handle most of the damage control during a major shipboard conflagration. [Ref 2]

With such a revolutionary manning requirement, designers of DD-21 will be able to utilize this study in order to ensure the automated DD-21 damage control system is able to handle any scenario.

B. PREVIOUS WORK

In the late 1980's, Jones and Foley [Ref 3] developed CFAST, a deterministic model which added greater versatility to the zone model. A zone model is a tool which simplifies the complex problem of modeling fire in a space. The most important advance that CFAST made over previous works in the field was that the conservation equations were solved in their original differential form. For each zone (also called control volume), a set of conservation equations was the beginning point. The conservation equations were recast in predictive equations for variables being observed (e.g. temperature, pressure, density, etc. in the compartment). The predictive equations were derived from the conservation equations, the equation of state and the boundary and initial conditions of the space. The result was a set of ordinary differential equations that used the physical quantities of mass and energy as their forcing functions. Multiple compartments were modeled and then each compartment was divided into two zones, a relatively hot upper layer and a relatively cool lower layer. Some of the approximations made were that temperature and density were uniform throughout a control volume and that pressure is approximately uniform in the compartment.

Among the different situations considered in this study were horizontal flow and vertical flow due to natural body forces; forced flow resulting from ventilation; and radiation effects.

Jones and Walton [Ref 4] applied the zone model concept specifically to a *Oliver Hazard Perry*-class frigate, the same class of ship as the USS *Stark*. The purpose of the study was to see if previous models of fires in buildings could be applied to a shipboard fire environment. The scenario used a one megawatt fire caused by a light missile whose warhead did not detonate. The principal differences between a building fire and shipboard fire recognized by this study were that ships have vertical scuttles and ladders which become the primary means of firefighters' movements during a shipboard fire and that slow burning rocket fuel produced a high density solid carbon waste product. These differences were accounted for in the multiple compartment model, and the same numerical methods developed in Reference 3 were applied without the use of the CFAST software. The authors concluded that models developed to predict the propagation of smoke and fire in buildings could be applied to ships with only a few modifications.

Mehls [Ref 5] used CFD-ACE, a fluid flow software developed by CFD Research Corporation to model shipboard fire and smoke. He developed a model of a passageway of an *Arleigh Burke*-class destroyer and simulated several smoke scenarios on a desktop computer. All three of Mehls' scenarios involved smoke entering a space at a fixed velocity, flowing through the space, and leaving the space at a fixed pressure. He neglected buoyancy effects caused by gravity.

Most recently, Tatem and Williams [Ref 6] used the zone model approach to study propellant-initiated fires. The authors used FAST as opposed CFAST to model their fire scenarios. FAST, the predecessor to CFAST, was more appropriate in this case because FAST allows the engineer to prescribe the heat release history of a fire regardless of the available oxygen in the compartment. Since propellant includes its own oxidizer,

this option was very essential to this study. Once the authors completed their propellant fire simulations, they compared their results with test data compiled during hull vulnerability (HULVUL) tests conducted on an ex-*Leander*-class Royal Navy frigate. Results of the simulations were in excellent agreement with those of the HULVUL tests.

C. OBJECTIVES

The purpose of this study is to model a vital shipboard space using a software package that has not been widely used in the field of smoke and fire propagation. The location of the modeled compartment has been carefully chosen in order to attempt to anticipate the effect of smoke and heat on damage control parties accessing or transiting the compartment. In addition to smoke properties observed in previous studies, heat transfer resulting from a heat source within the modeled space will be examined.

THIS PAGE INTENTIONALLY LEFT BLANK

II. COMPUTATIONAL FLUID DYNAMICS

A. OVERVIEW

The software used in this study is CFD-ACE+ developed by CFD Research corporation. CFD-ACE+ provides an advanced computational environment for the analysis of fluid flow and heat transfer for a wide variety of engineering applications. The objective of CFD-ACE+ is to make the study of computational fluid dynamics easier for the user who is not well-versed in the numerical methods necessary to analyze complex fluid flow and heat transfer problems. [Ref 7]

There are three distinct steps in the process for a typical numerical solution. First, the solution space must be divided in one or more problem domains. Next, a grid is applied to the problem domain. Then, the equations, boundary conditions, and initial conditions that need to be solved at each cell must be formulated. In addition, the numeral technique to be utilized must be stipulated. Finally, once the solution is complete, the data must be processed and displayed in a form that is useful to the engineer. CFD-ACE+ has several tools available to perform each of these steps, but only those used in this study will be discussed.

The CFD-ACE+ component used for geometry construction and grid generation is CFD-GEOM. Similar to other computer aided design (CAD) packages, CFD-GEOM provides the tools necessary for the engineer to create the problem domain. Once the geometry of the problem domain is constructed, grids are generated and the problem domain is discretized into individual cells or control volumes over which the flow equations are integrated. There are two classes of cells that can be generated in CFD-GEOM: structured and unstructured. [Ref 7]

CFD-ACE(U) is the flow solver for unstructured, polyhedral cells. It utilizes CFD-GUI, an advanced graphical user interface, to specify the physics of the problem, the differencing scheme to be used, and the boundary and initial conditions of the discretized equations. CFD-ACE(U) also includes a wide variety of physics modules that can be used for more complicated problems. Some of the modules being used in this study, are the flow module, the heat transfer module and the mixing module. [Ref 7]

Once the problem has been processed through CFD-ACE(U), CFD-VIEW sorts through the large volumes of data, and allows the user to display the results in a useful graphical format. Any parameter solved for in CFD-ACE(U) can be displayed as a surface. Some of these surfaces include constant computational plane surfaces, cutting plane surfaces and isosurfaces. [Ref 7]

B. FINITE VOLUME METHOD

1. Basic Governing Equations

CFD-ACE employs the finite volume method in order to integrate the fluid mechanics governing. [Ref 8] The following passage summarizes the CFD-ACE approach to the integration of the governing equations over the problem domain.

In CFD-ACE methodology, fluid flows are simulated by numerically solving partial differential equations that govern the transport of flow quantities also known as flow variables. These variables include mass, momentum, energy, turbulence quantities, mixture fractions, species concentrations, and radiative heat fluxes. The variables for which transport equations have to be solved will depend on the nature of the flow problem. [Ref 8]

CFD-ACE employs conservative finite-volume methodology and accordingly all the governing equations are expressed in conservative form. Cartesian coordinate system and tensor notations are generally employed in which repeated indices imply summation over all coordinate directions. [Ref 8]

The partial difference equations discussed in the above passage and their derivations can be found in Chapter 2 of Ref. 8.

2. Discretization Methods

In order to numerically solve the partial differential equations discussed in the previous section, they must be discretized over computational grid, be formed into algebraic equations and then solved. The numerical method results in a discrete solution of the problem domain in terms of the flow variables at the grid points. The problem domain is made up of a number of cells known as control volumes. See Figure 2. The CFD-ACE method of discretizing the governing equations will not be presented here but a detailed explanation can be found in Ref. 8. Once all the all the discretized equations derived in the preceding sections are combined, Equation (2-1) will result.

$$a_p \phi_p = a_w \phi_w + a_e \phi_e + a_s \phi_s + a_n \phi_n + a_l \phi_l + a_h \phi_h + a_{sw} \phi_{sw} + a_{se} \phi_{se} \\ + a_{nw} \phi_{nw} + a_{ne} \phi_{ne} + a_{ls} \phi_{ls} + a_{ln} \phi_{ln} + a_{hs} \phi_{hs} + a_{hn} \phi_{hn} + a_{wl} \phi_{wl} \\ + a_{wh} \phi_{wh} + a_{el} \phi_{el} + a_{eh} \phi_{eh} + S_u \quad (2-1)$$

Equation (2-18) is the finite difference equation (FDE). The ϕ 's are the flow variables (i.e. velocity, enthalpy, pressure, etc.) and the coefficients a_p , a_w , etc. are known as link coefficients. Since the link coefficients are functions of their respective ϕ 's (i.e. a_w is a function of ϕ_w , and so forth), the FDE is nonlinear. This quote from Ref. 8 best explains how CFD-ACE manipulates the FDE.

When an FDE is formulated for each computational cell, it results in a set of coupled nonlinear algebraic equations. No direct matrix inversion method is available to solve a set of nonlinear algebraic equations. Therefore an iterative procedure is employed in CFD-ACE at every time step. A linear FDE is formed by evaluating the link coefficients with the values of ϕ available at the end of the previous iteration.

$$\alpha_p^k \phi_p^{k+1} = \sum \alpha_{nb}^k \phi_{nb}^{k+1} + S_U^K \quad (3-31)$$

Here, the compact notations α_{nb} and ϕ_{nb} are used to represent the link coefficients and the values of the flow variable corresponding to the neighboring grid points. The superscripts k and $k+1$ denote the previous and current iteration numbers respectively. When the linear set equation 3-31 is solved, we have an improved estimate for ϕ . This improved estimate is used to update the link coefficients α_p , α_{nb} and S_U and the linear set is solved again. The iterative procedure is repeated until a converged solution is obtained. [Ref 8]

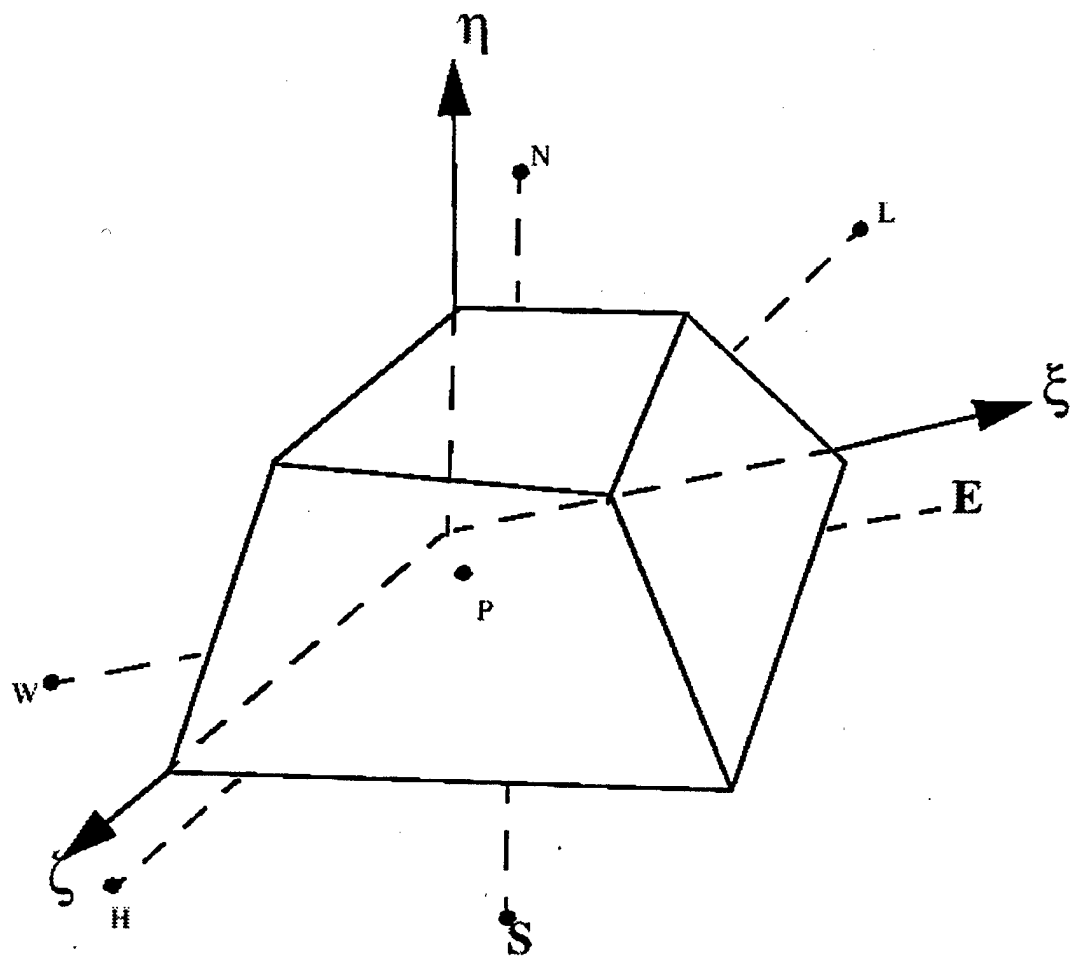


Figure 2. Schematic of Three Dimensional Body-fitted Coordinate System Control Volume. [Ref. 8].

THIS PAGE INTENTIONALLY LEFT BLANK

III. MODEL

A. GEOMETRY

1. Model Selection

The space modeled for this study was passageway 1-158-1-L, the outboard passageway at frame 158 on an *Arleigh Burke* (DDG-51)-class destroyer. See Figure 3. The reason for the selection of this space was the vital nature of its location with respect to the rest of the ship. It is one of the main passageways on the starboard side of the main or damage control deck. It is an essential passage for damage control parties, medical teams, or other personnel moving between the forward and aft sections of the ship. It's forward, inboard hatch (the door closest to the centerline of the ship) directly accesses the Combat Information Center, the ship's most significant space during a combat situation, and the source of much smoke and heat during the *Stark* incident. The space has four vertical water-tight hatches (doors), a horizontal hatch and scuttle in the overhead (ceiling), and a horizontal hatch and scuttle in the deck (floor). A ladder extends from the aft end of the lower horizontal hatch to the fwd end of the upper horizontal hatch at an angle of 53.9° with the deck. The ladder will not be modeled in this study because it will greatly increase the complexity of the problem. Figure 3 is a ship's drawing representation of passageway 1-158-1-L.

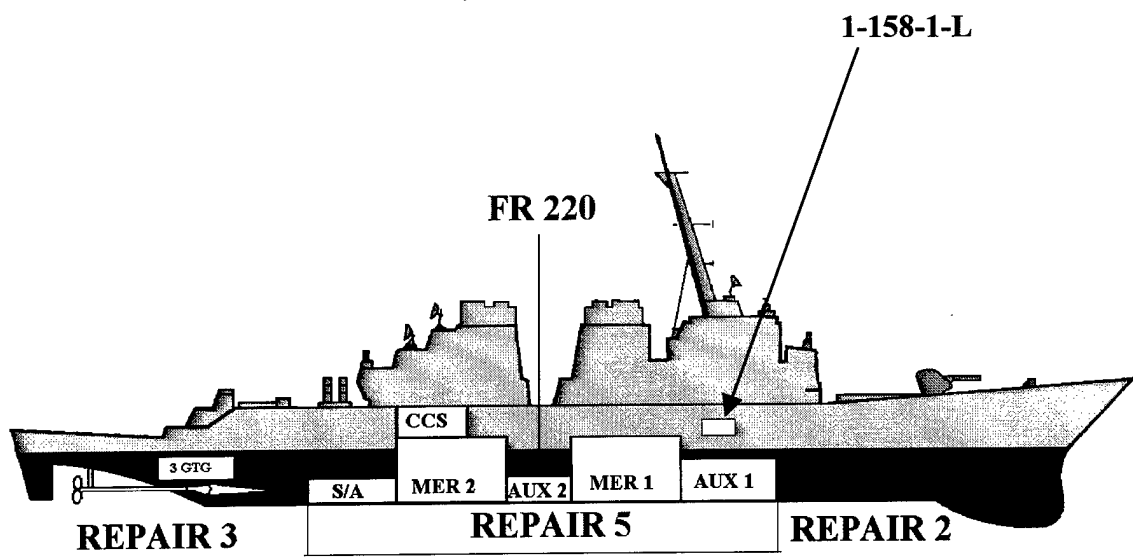


Figure 3. Starboard Side View of an *Arleigh Burke* (DDG-51) class destroyer, showing position of modeled space. [Ref. 10].

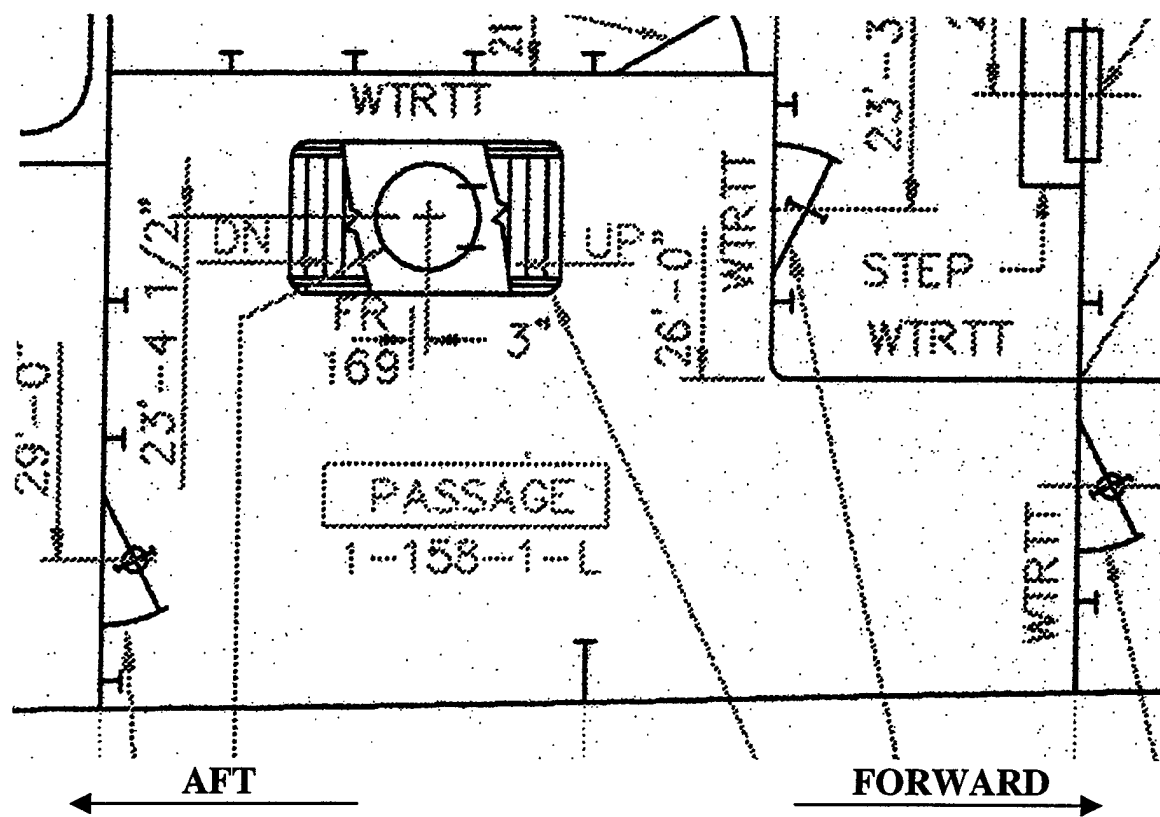


Figure 4. Ship's Drawing of Passageway 1-158-1-L.

2. Grid Distribution and Model Generation

The problem domain modeling and simulations for this study were carried out using a Micron Client Pro Desktop computer, with 384 megabytes of RAM and an internal hard drive with 12 gigabyte capacity. The software used was CFD-ACE version 6.2, which was last updated July 16, 2000.

The first step in studying a fluid flow heat transfer problem using CFD-ACE+ is to model the problem domain using CFD-GEOM. CFD-GEOM possesses most of modeling tools encountered in any Computer Aided Design (CAD) software. The problem domain was modeled using the exact specifications of the space taken from NAVSEA ships drawings. The outline of the problem domain is shown in Figure 4.

The next step was to apply a grid to the problem domain using the grid construction tools of CFD-GEOM. A combination of structured and unstructured grid formats was used in applying a grid to this problem domain. Structured grids are cells composed of standard six-sided cubes, while unstructured grid cells are tetrahedrons. The unstructured grid format facilitates grid generation and grid refinement.

The structured grids were done first. The structured grid hierarchy begins with edges. The outline of the two horizontal hatches, the overhead and the deck were made into edges. In CFD-GEOM, an edge is a set of lines consisting of a set of grid points. Once all the edges were complete, faces are the next step in the grid hierarchy. A face is formed by designating a set of four user-specified edges that form a closed two-dimensional region. Once a face is formed, a resulting grid called a face grid is formed.

For the unstructured grid section, the surface is the first object in the hierarchy. A surface is formed by choosing four or more lines or edges that enclose a two-dimensional

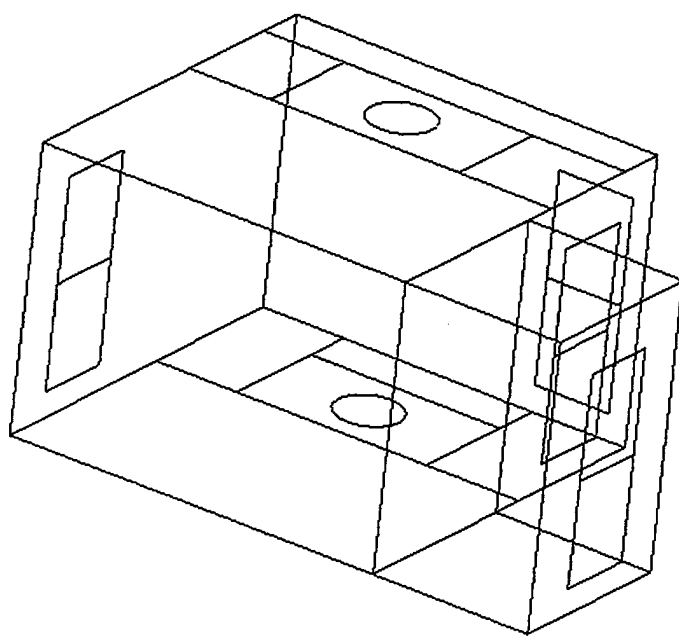


Figure 4. Outline of Problem Domain. CFD-GEOM model of 1-158-1-L.

region on which the unstructured surface grid is to be created. Once a surface is created, the loop is the next object in the hierarchy. A loop is formed by choosing the same lines or edges chosen for the surface. The loop defines the boundary of the two-dimensional surface to be gridded. The loop is then trimmed or coupled to the surface, forming a trimmed loop. The trimmed loop defines the active surface for unstructured surface gridding. The user must ensure that the arrows identifying the trimmed loop are pointing into the two-dimensional surface where the unstructured grid is needed. All vertical bulkheads (walls) were designated as trimmed loops. A trimmed loop was also formed at the interface between the forward “alcove” of the space and the wide section of the space. The scuttles and hatches were trimmed to a surface, and then designated a dual loop, so that an unstructured surface grid would be generated on the inside and outside portions of the designated entity. The user can identify dual loop by arrows pointing to both the inside and outside of the designated entity.

Once all face grids and loops were constructed, the next step was to construct a surface set. A surface set consists of a set of trimmed loops and faces that define an enclosed three-dimensional region. In this problem, two surface sets were created. The forward “alcove” area was one set and the aft wide section was another surface set. Once the surface sets were formed the next step in the hierarchy was domain creation. The domain defines the volume where the unstructured grid will be created. The domain is created by selecting all the previously created surface sets. Once the domain is formed, the unstructured grid can be generated. Using the grid application of CFD-GEOM, first a unstructured face grid is generated. When the unstructured face grid is generated, the square two-dimensional structured face grids will be “cut” into triangular surface grids,

and triangular surface grids will be created on the two-dimensional surfaces bounded by the trimmed loops. Figure 5 shows the unstructured face grid for the problem domain being studied here.

The final step in CFD-GEOM is the creation of the unstructured volume grid. Choosing the tetrahedron grid icon, and then selecting the domain will create an unstructured grid. For this problem, once the unstructured grid was formed there were unusually large tetrahedrons in the center of the problem domain. This problem was solved by creating two volume sources and placing them in the center of the problem domain. The volume sources solved the problem of the large grid cells by forcing the grid cells closer together. The final grid cell count for this model was 154,621.

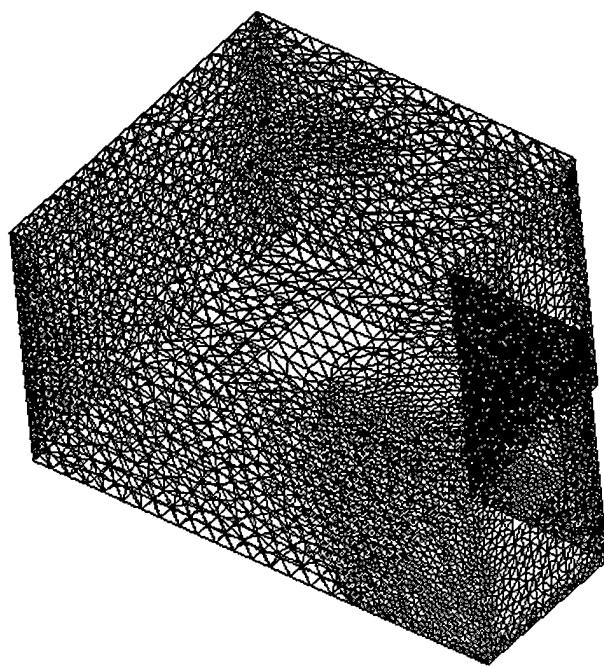


Figure 5. Face Grid On Model of 1-158-1-L.

B. THERMOPHYSICAL MODEL

Once the problem domain has been modeled and the grid has been created in CFD-GEOM, the problem is then sent to the solver. CFD-ACE+ possesses a number of solvers. The one used in this study was CFD-ACE(U), the unstructured, polyhedral cell flow solver. CFD-ACE(U) contains many modules dealing with fluid flow and heat transfer. The modules used in this study were the flow module, the heat transfer module, the turbulence model, and the chemistry module. For this problem, the chemistry model was used only simulate the mixing of smoke and air, and not to simulate any chemical reactions. CFD-ACE(U) interfaces with CFD-GUI which is tool used to input problem type, and boundary and initial conditions.

The problem type to be solved in ACE(U) for the problem domain generated in CFD-GEOM was an incompressible flow, heat transfer problem. Turbulence and buoyancy effects were accounted for. In the flow module, the model chosen was the “no slip” condition for momentum and heat transfer, meaning all velocity components are set to zero (wall velocity) and the gas temperature is set to the wall temperature. In the heat transfer module, all bulkheads, the overhead and the deck were designated as isothermal surfaces. The wall temperature was maintained at a set value, and the heat flux needed to maintain the temperature was calculated by CFD-ACE(U). In the turbulence module, the model chosen was the Low Reynolds Number $k - \varepsilon$ Model of Chien (1982). For details on the turbulence model, see Ref. 9. In the chemistry module, the Mixture Mass Fractions option was used to model the mixing of air and smoke.

C. ADDITIONAL INPUTS

In order to ensure convergence of the problem, several inputs specific to CFD-ACE + and used in this study will be discussed. For the initial conditions, a velocity slightly lower than the input velocity was entered. While seemingly unrealistic, the initial velocity inside the space provided stability to the problem.

Under-relaxation constrains the change of a dependent or auxiliary variable from one iteration to the next. In this study, the under-relaxation parameters were slightly increased for enthalpy, turbulence, and pressure. See Appendixes for specific values. Increasing the under-relaxation settings adds stability to the problem, but will result in slower convergence.

IV. RESULTS

Three successful scenarios were simulated utilizing this model. A successful scenario is defined in the CFD-ACE manuals, as the residuals of the problem converging at least 5 orders of magnitude. Also, the mass flow and heat transfer summaries must be at least two orders of magnitude below zero. [Ref 8]

Scenario A (see Appendix A) is the control scenario of this study. Mehls [Ref 5] Scenario A was recreated using a different space geometry, a different grid type, and updated software. With the exception of obvious differences, the results of this scenario were in excellent agreement with Mehls. The results of Scenario A showed that Mehls work could be expanded to a larger space. Figure 6 is a colorized version of the model outline showing the designated inlet and outlet of the space. Figures 7 through 11 are various isosurfaces showing different concentrations of smoke and air for direct comparison to Mehls work.

Scenario B was identical to Scenario A with the addition of buoyancy effects added by activating the gravity term in CFD-ACE(U). The addition of buoyancy complicated the problem greatly and significantly increased the time required for one simulation. However, once the simulation was complete, the results showed significant differences from those of Scenario A. The introduction of gravity in the problem appears to increase smoke propagation into the space. See Appendix B. Figure 12 is a colorized version of the model outline showing the designated inlet and outlet of the space. Figure 13 is a Z-cut with vectors showing the warmer, lighter smoke/air mixture being driven into the overhead. Figure 14 is a Z-cut which shows that the space is dominated by a smoke/air mixture that is at least 75% smoke concentration by volume. Figure 15 shows

an X-cut and Y-cut displaying the temperature distribution in the space. Figure 16 is an X-cut showing the density distribution in the space near the inlet. Figure 17 shows an isotherm of 75% smoke concentration by volume.

Scenario C was completed in order to observe the effects of a heat source. An attempt was made to use the wall source option in the CFD-ACE(U). However, the results were inconsistent, and not enough information on how CFD-ACE(U) handles the wall source option were available in the CFD-ACE+ manuals. More specific knowledge on the wall source option is required before it can be used in smoke propagation simulations. Instead, the deck of the space was designated as an isothermal surface at 1200K. This scenario was compared with Mehls Scenario C. This study concurs with Mehls findings that the heated deck does not affect smoke propagation. However, the isothermal layers rising from the deck are much thinner than in Mehls Scenario. See Figures 19 and 20. This decrease in the size of the layers could possibly be due to the introduction of gravity into the problem. Figure 18 is a colorized version of the outline of the model with the inlet, outlet, and heated deck highlighted. Figure 19 shows an X-cut and Y-cut displaying the effect of the heated deck on the temperature distribution in the space. Figure 20 shows an isosurface of 96% smoke concentration by volume and the effect of this heated deck on this particular smoke/air mixture. Figure 21 is an isosurface of 13% air smoke concentration. The air concentration of 13% is fairly large for the buoyancy problems in this study. Note how the heated deck does not effect this particular concentration.

V. CONCLUSIONS

This study was successful in increasing the size of the space studied, and observing the effects of buoyancy that were not observed in previous works. It was also discovered that the larger and more non-symmetrical a space gets the more difficult it is to model a space using the structured grid format. The unstructured grid format greatly facilitates both grid creation and grid refinement. The model design, including grid creation, for this study was completed in at least half the time it would have taken to complete the task using structured grid format. The addition of gravity in order to study buoyancy effects also necessitated the use of an unstructured grid. The smoke propagation problem with buoyancy included required a finer grid, and the refinement of the grid was completed in minutes. The finer grid also meant longer simulation times. Scenarios B & C took more than twelve hours to complete. The plans for this research originally included attempts at time-based scenarios. However, the current scenarios using the current model and using the time-dependence option would take 120 hours for 10 time steps.

VI. RECOMMENDATIONS

The following recommendations are made for the continuation of this study.

- In CFD-GEOM, designate the cells adjacent to the walls as the actual material used aboard the *Arleigh Burke* (DDG-51) class destroyer. This will create a more realistic simulation.

- Further investigate the wall source option in CFD-ACE(U). This setting should provide more accurate results than the isothermal surface at 1200K.

- Model one space on top of another. In CFD-ACE(U) designate the surface between the two as a wall with external heat transfer due to convection and radiation. Study the effects of a heat source in the lower space on the upper space.

- Model a smaller space in order to use the transient option of CFD-ACE(U) to run time-based scenarios.

APPENDIX A

Appendix A was the control scenario. Mehls [Ref 5] Scenario A was recreated using a different grid structure and different space. The results show good agreement with Mehls, with there being exceptions due to the different size and shape of the model.

Relaxation	Velocity	(m/s)	0.3
	Turbulence	(J)	0.5
	Enthalpy	(KJ/kg)	0.06
	Pressure Correction	(Pa)	0.07
	Mixture Fractions		0.3
Initial Conditions	Air		
	U Velocity	(m/s)	-0.1
	V Velocity	(m/s)	0
	W Velocity	(m/s)	0
	Relative pressure	(Pa)	0
	Turbulence Dissipation Rate	(J/kg·s)	0.923
	Turbulence Kinetic Energy	(m ² /s ²)	0.098
	Temperature	(K)	300
	Reference Pressure	(Pa)	1E5
Boundary Conditions	Isothermal Wall Temperature	(K)	300
Inlet – Smoke	U Velocity	(m/s)	-0.1
Top	V Velocity	(m/s)	0
	W Velocity	(m/s)	0
	Temperature	(K)	500
	Turbulence Kinetic Energy	(m ² /s ²)	0.098
	Turbulence Dissipation Rate	(J/kg·s)	0.923
	Pressure	(Pa)	0
Inlet - Air	U Velocity	(m/s)	-0.1
Bottom	V Velocity	(m/s)	0
	W Velocity	(m/s)	0
	Temperature	(K)	500
	Turbulence Kinetic Energy	(m ² /s ²)	0.098
	Turbulence Dissipation Rate	(J/kg·s)	0.923
	Pressure	(Pa)	0

Table 1. CFD-GUI inputs for Scenario A.

Outlet	U Velocity	(m/s)	0
	V Velocity	(m/s)	0
	W Velocity	(m/s)	0
	Temperature	(K)	400
	Turbulence Kinetic Energy	(m ² /s ²)	0.098
	Turbulence Dissipation Rate	(J/kg·s)	0.923
	Pressure	(Pa)	0

Table 1. Continued.

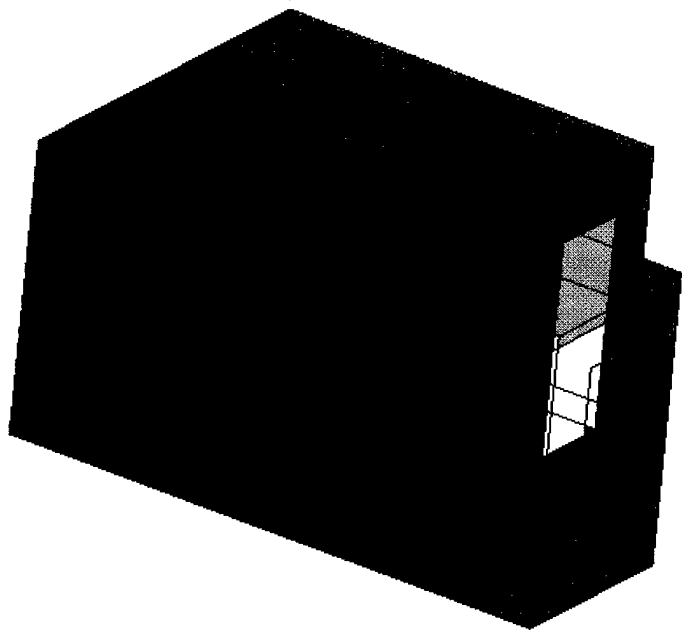


Figure 6. Outline of Model Showing Designated Inlets and Outlet.

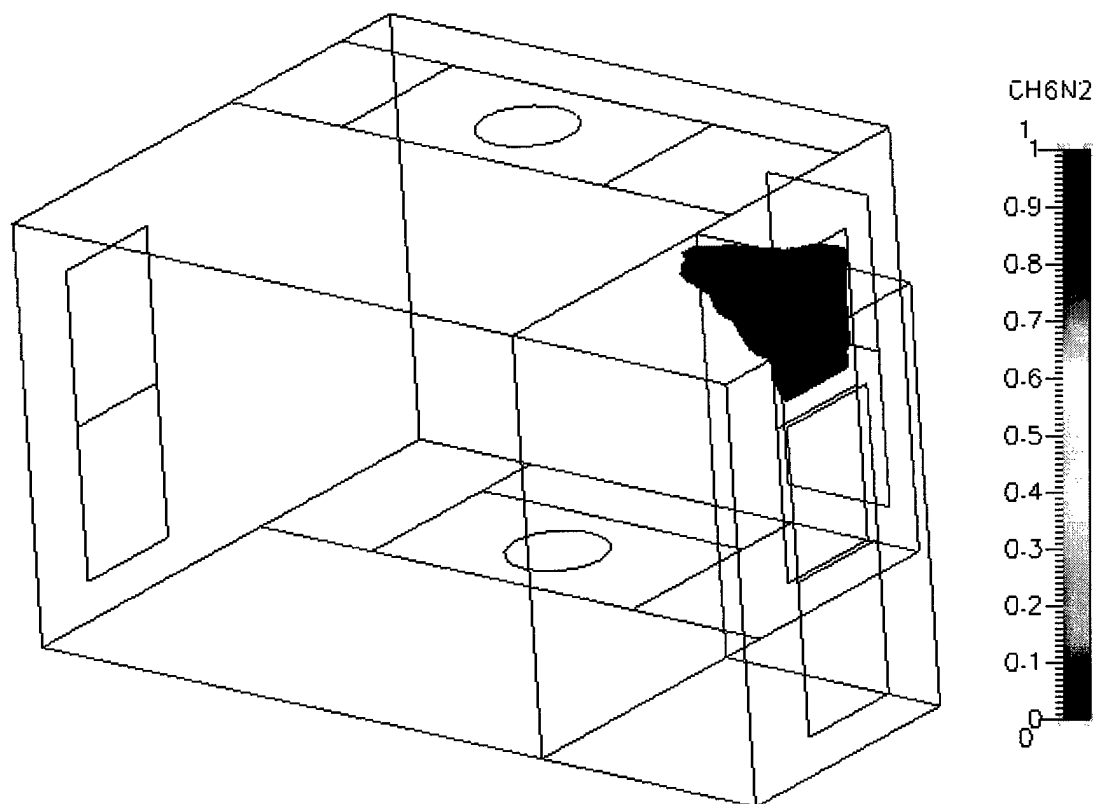


Figure 7. CFD-VIEW Representation Showing 98% Concentration of Smoke by Volume.

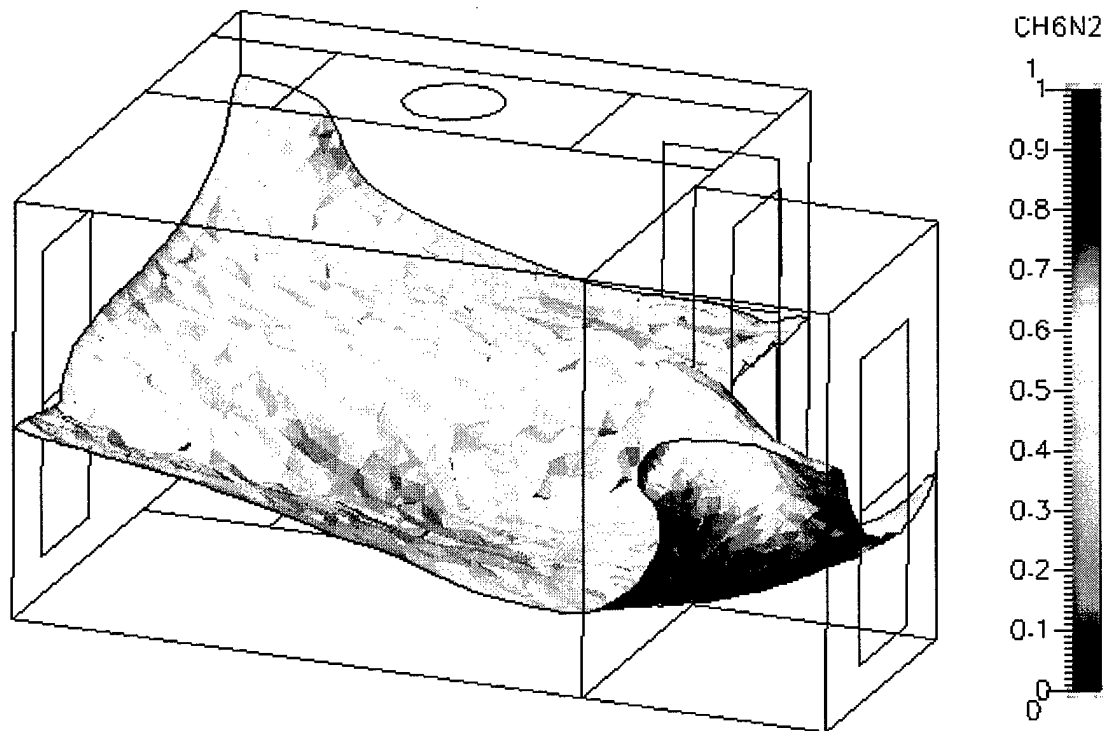


Figure 8. CFD-VIEW Representation Showing 54% Concentration of Smoke Volume.

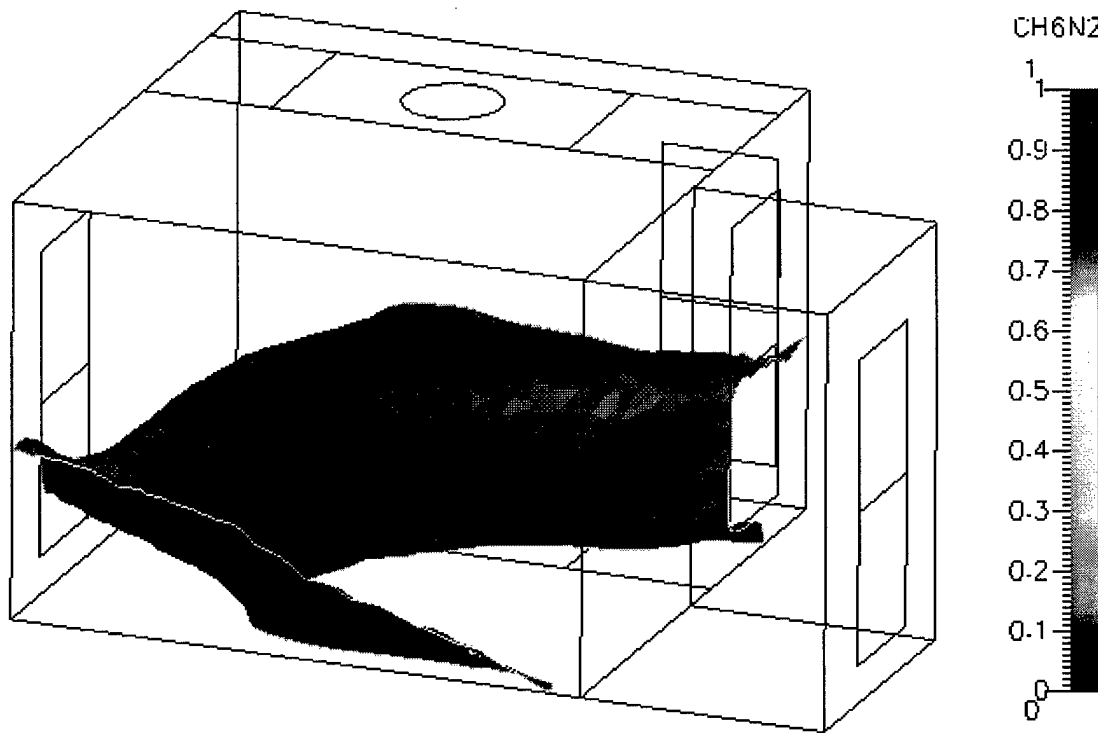


Figure 9. CFD-VIEW Representation of Showing 77% Concentration of Air by Volume.

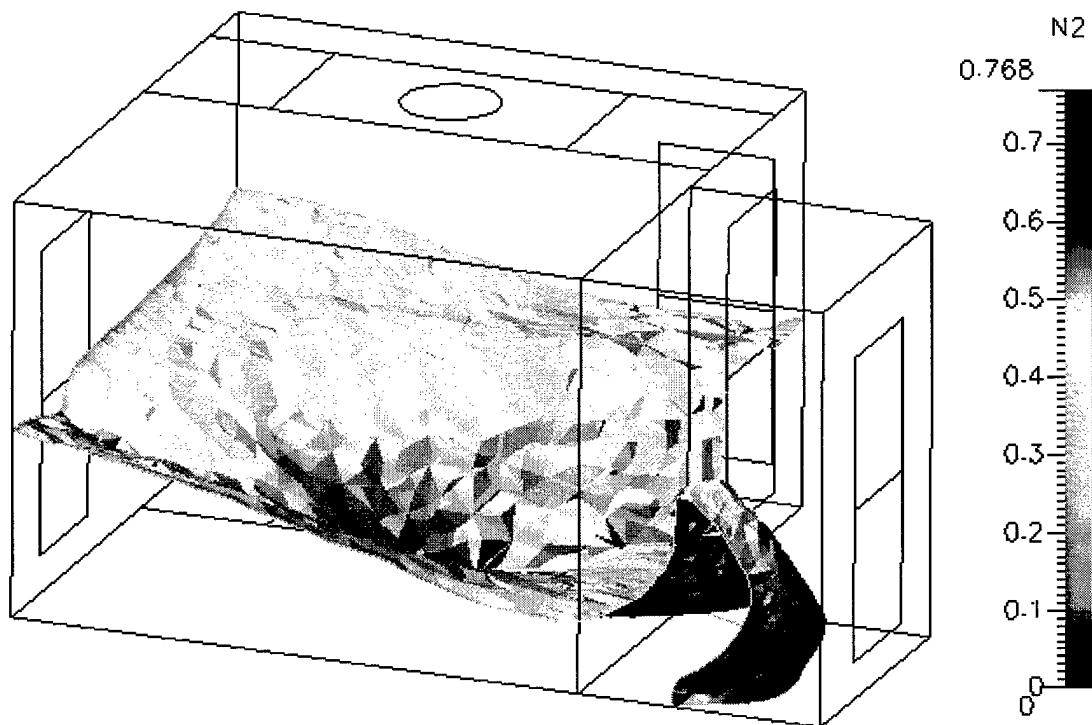


Figure 10. CFD-VIEW Representation Showing 54% Concentration of Air by Volume.

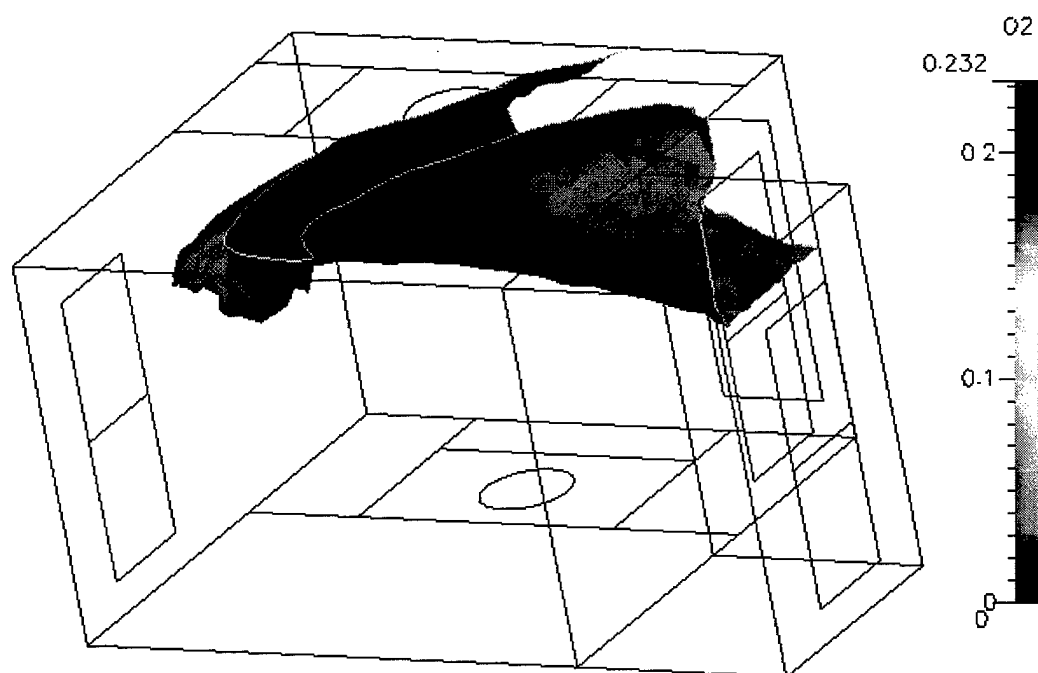


Figure 11. CFD-VIEW Representation Showing 16% Concentration of Air by Volume.

APPENDIX B

Scenario B is identical to Scenario A with the exception that buoyancy is included in Scenario B.

Relaxation	Velocity	(m/s)	0.3
	Turbulence	(J)	0.5
	Enthalpy	(KJ/kg)	0.06
	Pressure Correction	(Pa)	0.07
	Mixture Fractions		0.3
Initial Conditions	Air		
	U Velocity	(m/s)	-0.1
	V Velocity	(m/s)	0
	W Velocity	(m/s)	0
	Relative pressure	(Pa)	0
	Turbulence Dissipation Rate	(J/kg·s)	0.923
	Turbulence Kinetic Energy	(m ² /s ²)	0.098
	Temperature	(K)	300
	Reference Pressure	(Pa)	1E5
Boundary Conditions	Isothermal Wall Temperature	(K)	300
Inlet – Smoke	U Velocity	(m/s)	-0.1
Top	V Velocity	(m/s)	0
	W Velocity	(m/s)	0
	Temperature	(K)	500
	Turbulence Kinetic Energy	(m ² /s ²)	0.098
	Turbulence Dissipation Rate	(J/kg·s)	0.923
	Pressure	(Pa)	0
Inlet - Air	U Velocity	(m/s)	-0.1
Bottom	V Velocity	(m/s)	0
	W Velocity	(m/s)	0
	Temperature	(K)	500
	Turbulence Kinetic Energy	(m ² /s ²)	0.098
	Turbulence Dissipation Rate	(J/kg·s)	0.923
	Pressure	(Pa)	0

Table 1. CFD-GUI inputs for Scenario A.

Outlet	U Velocity	(m/s)	0
	V Velocity	(m/s)	0
	W Velocity	(m/s)	0
	Temperature	(K)	400
	Turbulence Kinetic Energy	(m ² /s ²)	0.098
	Turbulence Dissipation Rate	(J/kg·s)	0.923
	Pressure	(Pa)	0

Table 1. Continued.

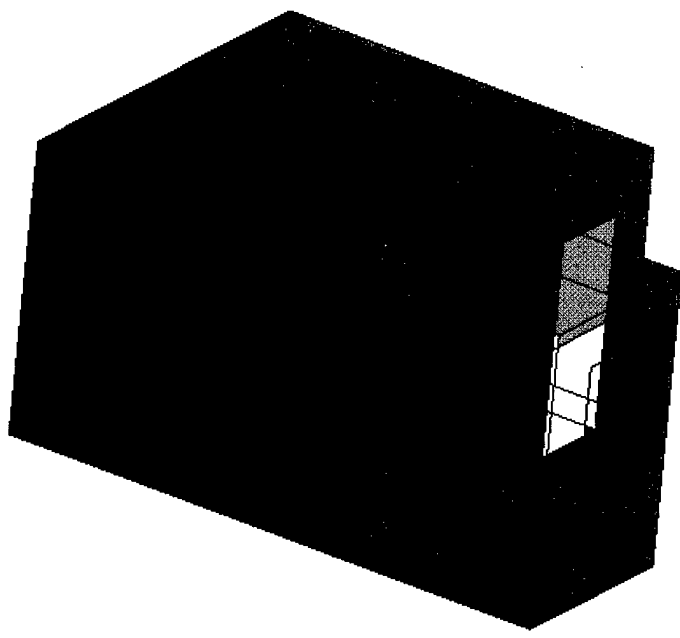


Figure 12. Outline of Model Showing Designated Inlets and Outlet.

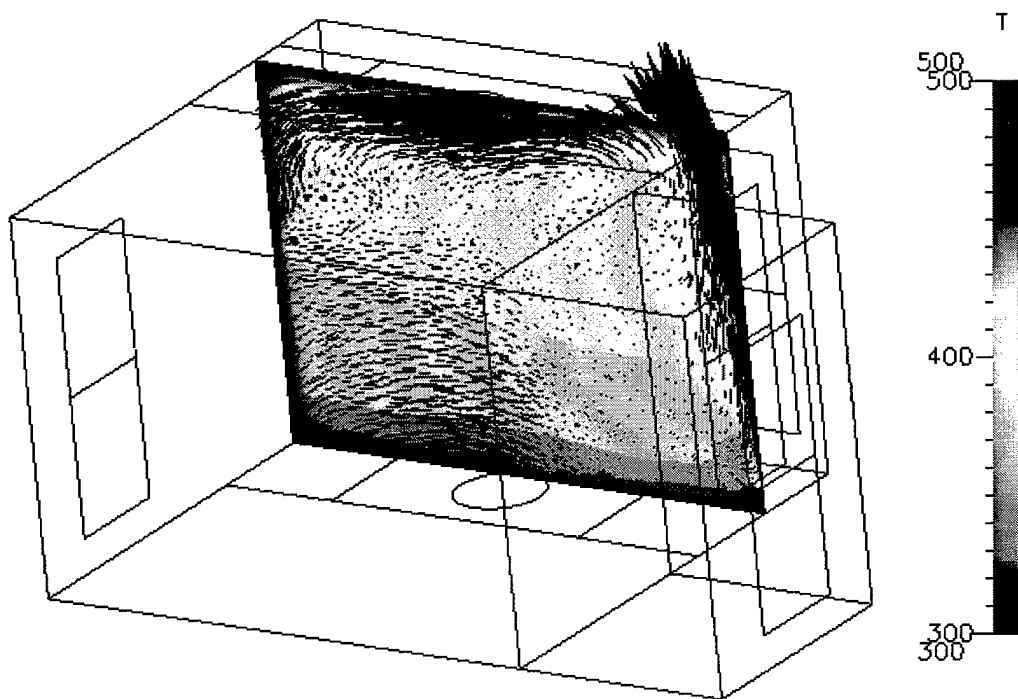


Figure 13. CFD-VIEW Representation Showing Warmer Lighter Air Being Driven into Overhead.

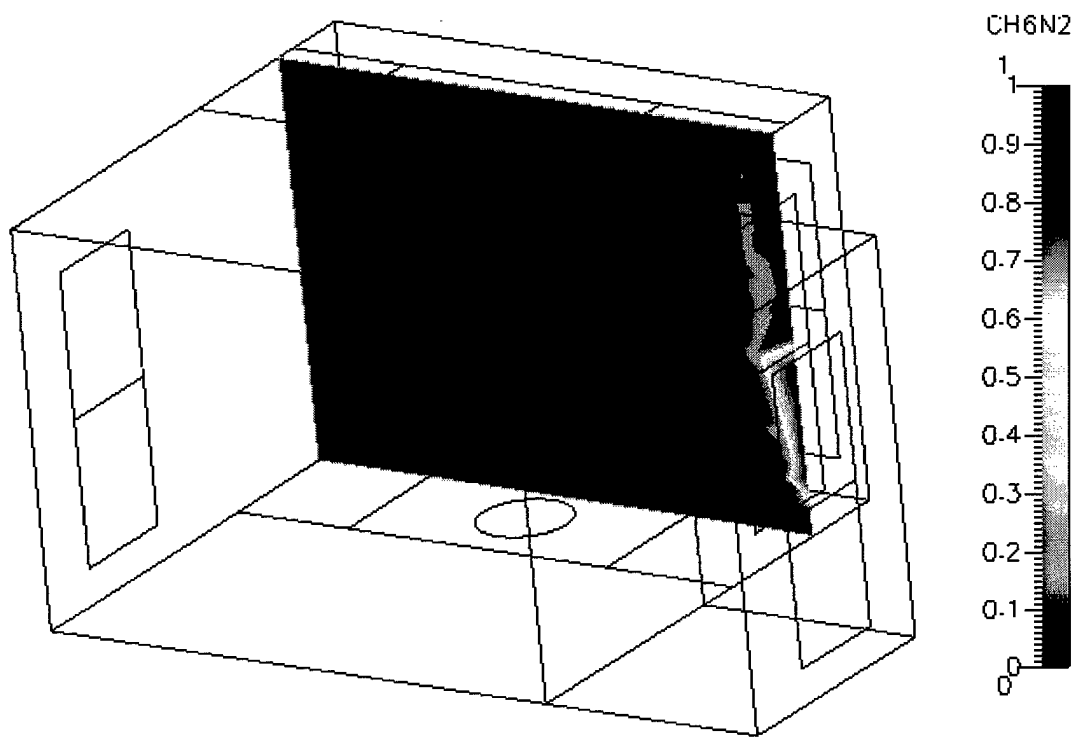


Figure 14. CFD-VIEW Representation Showing At Least 75% Smoke Concentration in Space.

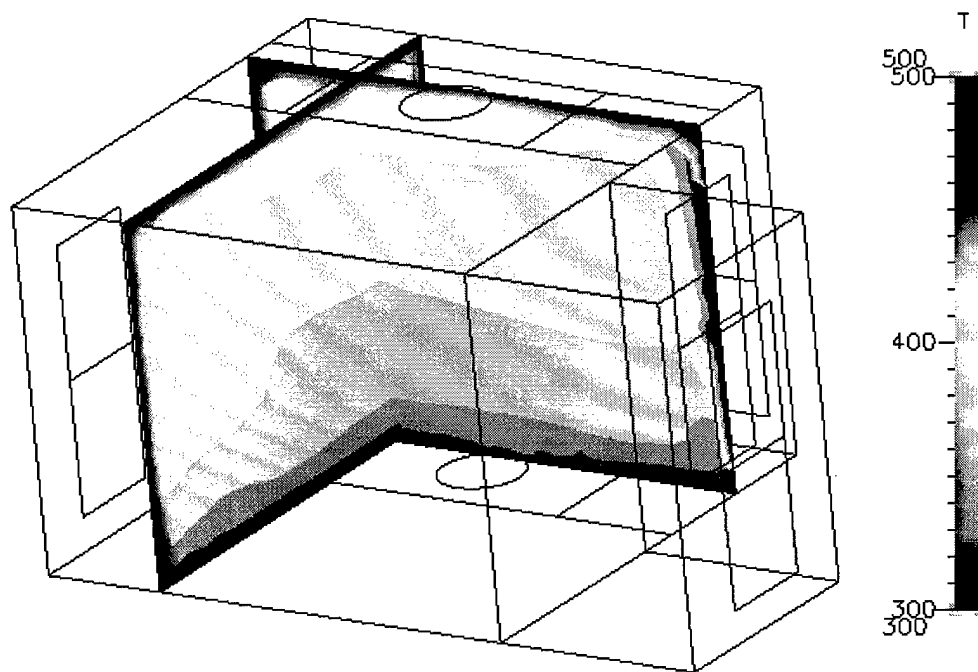


Figure 15. X-cut and Y-cut Showing the Temperature Distribution Within the Space.

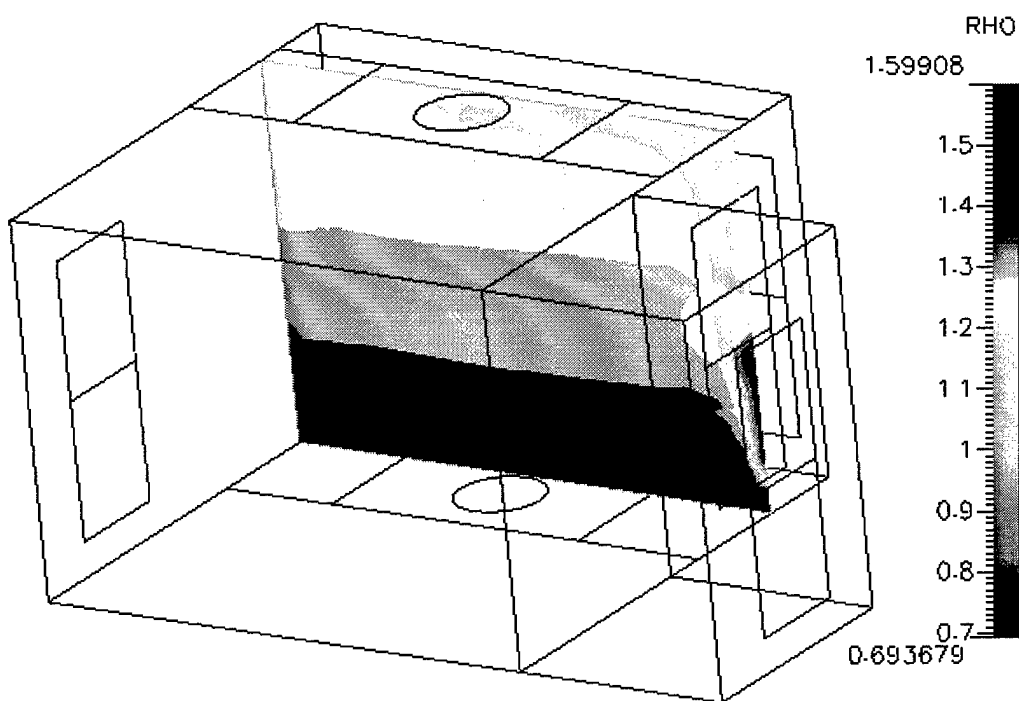


Figure 16. X-cut Showing Density Distribution in Space.

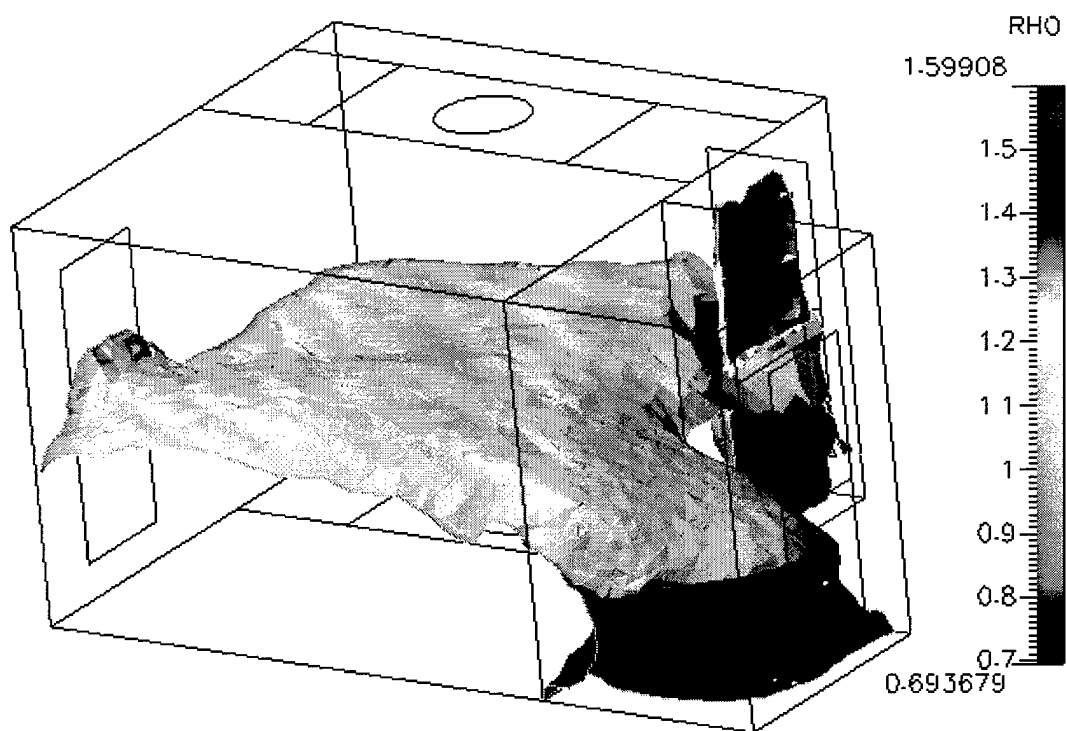


Figure 17. CFD-VIEW Representation Showing 75% Concentration of Smoke by Volume.

APPENDIX C

Appendix C includes the data from Scenario C. Scenario C designates the deck as an isothermal surface of 1200K.

Relaxation	Velocity	(m/s)	0.3
	Turbulence	(J)	0.5
	Enthalpy	(KJ/kg)	0.06
	Pressure Correction	(Pa)	0.07
	Mixture Fractions		0.3
Initial Conditions	Air		
	U Velocity	(m/s)	-0.1
	V Velocity	(m/s)	0
	W Velocity	(m/s)	0
	Relative pressure	(Pa)	0
	Turbulence Dissipation Rate	(J/kg·s)	0.923
	Turbulence Kinetic Energy	(m ² /s ²)	0.098
	Temperature	(K)	300
	Reference Pressure	(Pa)	1E5
Boundary Conditions	Isothermal Wall Temperature	(K)	300
Inlet – Smoke	U Velocity	(m/s)	-0.1
Top	V Velocity	(m/s)	0
	W Velocity	(m/s)	0
	Temperature	(K)	400
	Turbulence Kinetic Energy	(m ² /s ²)	0.098
	Turbulence Dissipation Rate	(J/kg·s)	0.923
	Pressure	(Pa)	0
Inlet - Air	U Velocity	(m/s)	-0.1
Bottom	V Velocity	(m/s)	0
	W Velocity	(m/s)	0
	Temperature	(K)	300
	Turbulence Kinetic Energy	(m ² /s ²)	0.098
	Turbulence Dissipation Rate	(J/kg·s)	0.923
	Pressure	(Pa)	0

Table 1. CFD-GUI inputs for Scenario C.

Outlet	U Velocity	(m/s)	0
	V Velocity	(m/s)	0
	W Velocity	(m/s)	0
	Temperature	(K)	350
	Turbulence Kinetic Energy	(m ² /s ²)	0.098
	Turbulence Dissipation Rate	(J/kg·s)	0.923
	Pressure	(Pa)	0

Table 1. Continued.

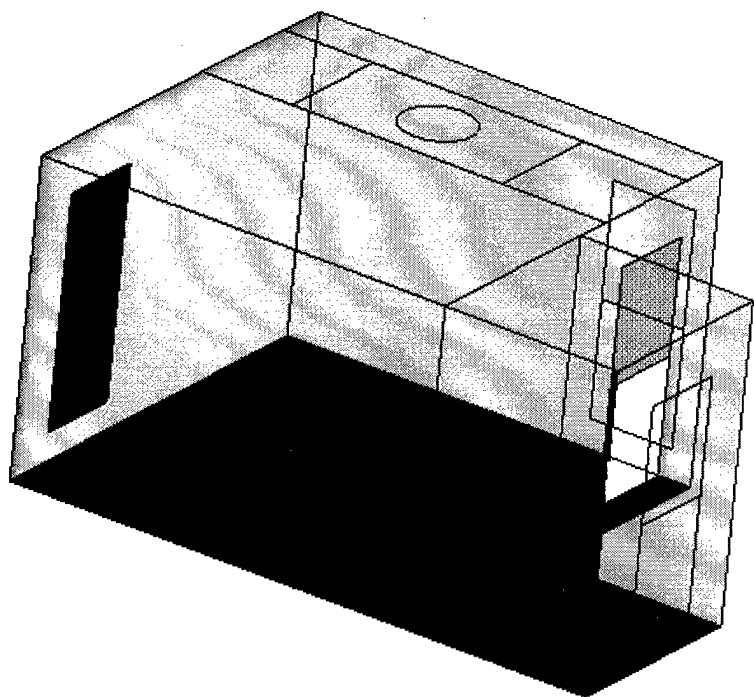


Figure 18. Outline of Model Showing Designated Inlets and Outlet and 1200K deck.

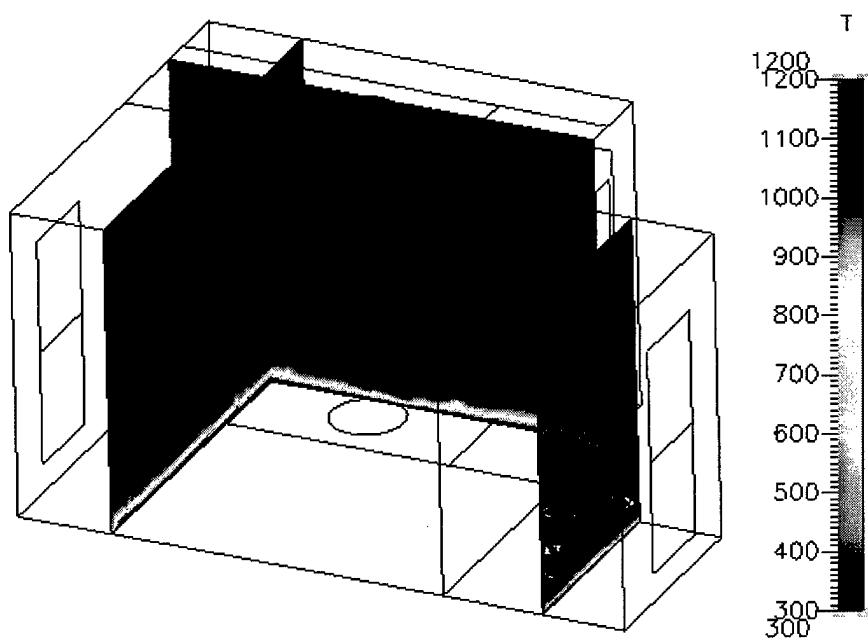


Figure 19. CFD-VIEW Representation Showing Effect of Heated Deck.

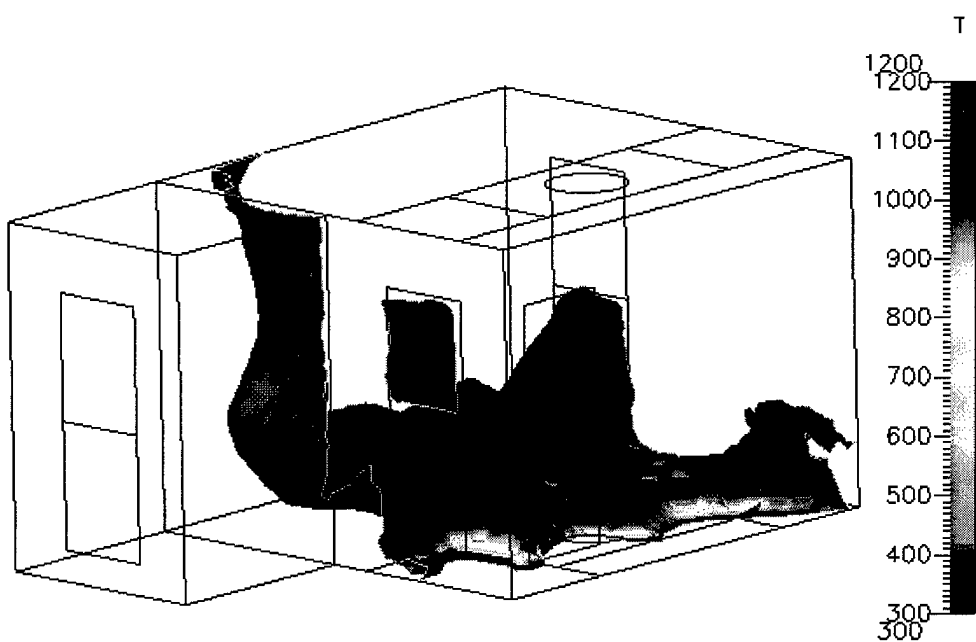


Figure 20. CFD-VIEW Representation Showing 96% Concentration Smoke by Volume.

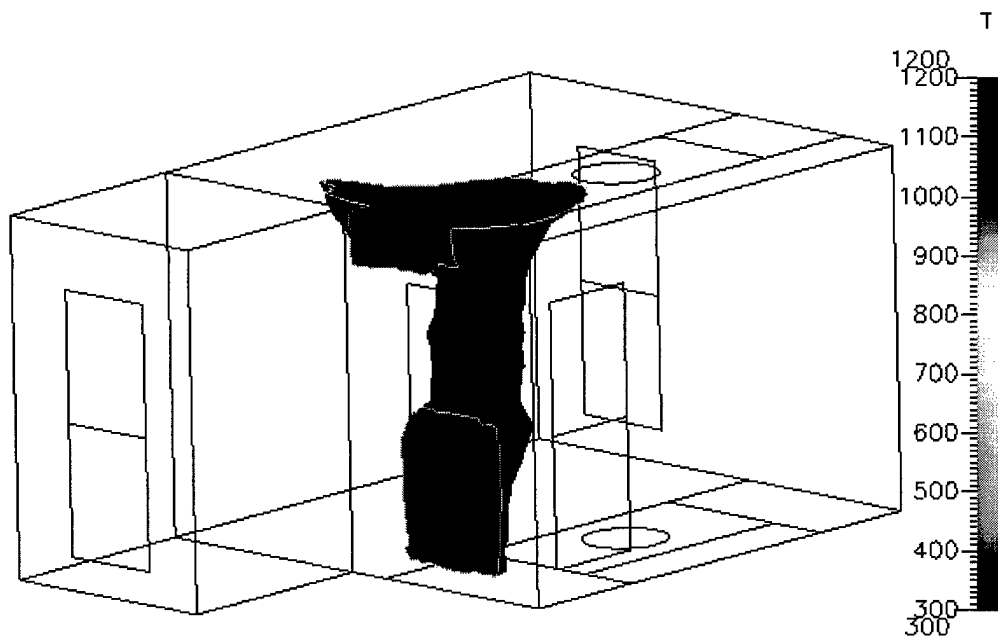


Figure 21. CFD –VIEW Representation Showing 13% Air Concentration by Volume.

LIST OF REFERENCES

1. Levinson, J., Edwards, R., *Missile Inbound*, Naval Institute Press, 1997.
2. Scott, R., "Ship Manpower: How Low Can We Go?", *Jane's Defence Weekly*, Volume 033, Issue 015, April 12, 2000.
3. Jones, W., Forney, G., *Modeling Smoke Movement Through Compartmented Structures*, National Institute of Standards and Technology Internal Report #4872, July 8, 1992.
4. Jones, W., Walton, W., *Spread of Smoke in an FFG-7*, Proceedings of the First NATO Conference on Fire Propagation Onboard Warships, Ottawa, Canada, 1983.
5. Mehls, M., *Propagation of Fire Generated Smoke in Shipboard Spaces*, M.S. Thesis, Mechanical Engineering Department, Naval Postgraduate School, March 2000.
6. Tatem, P., Williams, F., White, D., Beyler, C., *Modeling Missile Propellant Fires In Shipboard Compartments*, NRL/MR/6180-00-8446, March 30, 2000.
7. *Getting Started Guide*, Version 6.2, CFD Research Corporation, July 2000.
8. *CFD-ACE Theory Manual*, Version 5, CFD Research Corporation, October 1998.
9. *CFD-ACE(U), Modules*, Version 6.2, CFD Research Corporation, July 2000.
10. *Surface Warfare Officer Basic Engineering Division Officer Course Student Guide*, Volume 64a, December 1990.

THIS PAGE INTENTIONALLY LEFT BLANK

INITIAL DISTRIBUTION LIST

1. Defense Technical Information Center.....2
8725 John J. Kingman Road, Ste 0944
Ft Belvoir, Virginia 22060-6218
2. Dudley Knox Library.....2
Naval Postgraduate School
411 Dyer Road
Monterey, Ca 93943-5101
3. Engineering & Technology Curricular Office, Code 34.....1
Naval Postgraduate School
Monterey, Ca 93943-5101
4. Department of Mechanical Engineering Code ME.....1
Naval Postgraduate School
Monterey, Ca 93943-5101
5. Professor Matthew D. Kelleher.....2
Mechanical Engineering Department, Code ME/KK
Naval Postgraduate School
Monterey, Ca 93943-5101
6. LT B.J. Vegara, USN.....1
1414 S Elm St
Roswell, NM 88201
7. CFD Research Corporation.....1
Cummings Research Park
215 Wynn Drive
Huntsville, Alabama 35805
8. NAWC-Weapons Division.....1
Fire Research Office Code: 4B3100D
Attn: L. Bowman
China Lake, California 93555-6100

9. NAWC-Weapons Division.....1
Fire Research Office Code: 4B3100D
Attn: Jim Hoover
China Lake, California 93555-6100
10. NAVSEA 05P3.....1
Attn: Norm Yarbrough
2531 Jefferson Davis Highway
Arlington, VA 22242-5160
11. Dr. Evangelos Hytopoulos.....1
Manager, West Coast Branch
CFD Research Corporation
4962 El Camino Real
Suite 221
Los Altos, CA 94022
12. LT Mike Mehls.....1
NSWC
Dahlgren Division
Attn: Code C2E-MSO
17320 Dahlgren Rd
Dahlgren VA 22448-5100